How to cite: *Angew. Chem. Int. Ed.* **2020**, *59*, 14671 – 14676
International Edition: doi.org/10.1002/anie.202006570
German Edition: doi.org/10.1002/ange.202006570

Polymers

Spin Filtering Along Chiral Polymers

Suryakant Mishra, Amit Kumar Mondal, Eilam Z. B. Smolinsky, Ron Naaman, Katsuhiro Maeda,* Tatsuya Nishimura,* Tsuyoshi Taniguchi, Takumu Yoshida, Kokoro Takayama, and Eiji Yashima*

Abstract: *Spin-dependent conduction and polarization in chiral polymers were studied for polymers organized as self-assembled monolayers with conduction along the polymer backbone, namely, along its longer axis. Large spin polarization and magnetoresistance effects were observed, showing a clear dependence on the secondary structure of the polymer. The results indicate that the spin polarization process does not include spin flipping and hence it results from backscattering probabilities for the two spin states.*

Introduction

In recent years, it was established that when an electron is transmitted through chiral molecules one spin is preferred over the other. This effect is termed the chiral induced spin selectivity (CISS) effect and it results from the coupling between the linear momentum of the moving electron and its spin degree of freedom by the special symmetry properties of the chiral potential.[1] The CISS effect is observed in biomolecules like DNA,[2,3] peptides, and proteins[4] as well as in helicene,[5,6] chiral perovskites,[7] chiral polymers, and other molecules. In the case of polymers and supramolecular structures, several CISS related studies were performed. In the first case, a thin film of a chiral polymer was deposited on the surface and the magneto resistance effect was measured.[8] In another example, a working electrode coated with chiral molecules was used for enhancing hydrogen production in water splitting processes.[9] In a recent study, the effect of secondary chiral structures of supramolecular systems on spin-selective transmission was investigated and correlated with circular dichroism (CD) intensities for nanofiber-based materials.[10]

Whereas for most chiral molecules, the spin selectivity is measured when the molecules are adsorbed on a solid substrate and the measurements are performed along the main molecular axis (the longest dimension), perpendicular to the substrate plane, for polymers this configuration is problematic. Therefore, typically in the case of chiral polymers and wires, the measurements are conducted when the long axis of the molecules are in plane and the spin polarization is measured perpendicular to the molecular main axis (Figure 1 A). These measurements were necessarily lacking precision regarding the paths of the electrons in the film studied and they did not probe the effect of the polymer backbone on the spin polarization.

The present study aims to overcome the deficiencies in former studies of the CISS effect in polymers. Here polymers of well controlled length were adsorbed on a substrate when the long axis of the polymers is about perpendicular to the substrate plane (Figure 1 B). The spin polarization was measured for electrons transferred along the main axis of the polymer, hence probing the polymer backbone itself as a spin filter.

Originally the CISS effect was observed when electron transmission through chiral molecules was found to be spin dependent. However, later it was realized that the CISS effect results also in transient spin polarization, which is accompanied by charge polarization in chiral molecules. Namely, when the electric field is applied on a chiral molecule, or when a chiral molecule interacts with another molecule or with

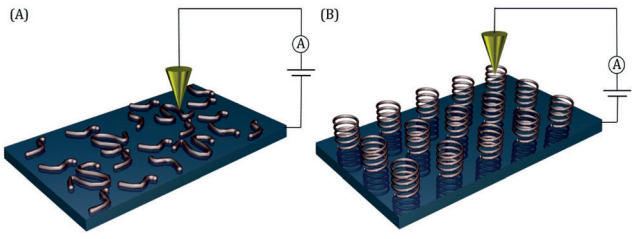

Figure 1. A) The typical configuration for spin-dependent electron transport through chiral polymers. In this case, the conduction perpendicular to the long axis of the polymer is measured. B) The configuration used in the current study, where the chiral polymers are organized as a self-assembled monolayer and the spin-dependent conduction is measured along the long axis of the polymer.

[*] S. Mishra, A. K. Mondal, E. Z. B. Smolinsky, R. Naaman
Department of Chemical and Biological Physics, Weizmann Institute
Rehovot 76100 (Israel)
E-mail: ron.naaman@weizmann.ac.il
K. Maeda
WPI Nano Life Science Institute (WPI-NanoLSI), Kanazawa University, Kakuma-machi, Kanazawa 920-1192 (Japan)
E-mail: maeda@se.kanazawa-u.ac.jp
K. Maeda, T. Nishimura, T. Taniguchi, T. Yoshida, K. Takayama
Graduate School of Natural Science and Technology, Kanazawa University, Kakuma-machi, Kanazawa 920-1192 (Japan)
E-mail: nishimura@se.kanazawa-u.ac.jp
E. Yashima
Department of Molecular and Macromolecular Chemistry, Graduate School of Engineering, Nagoya University
Chikusa-ku, Nagoya 464-8603 (Japan)
Supporting information and the ORCID identification number(s) for the author(s) of this article can be found under: https://doi.org/10.1002/anie.202006570.

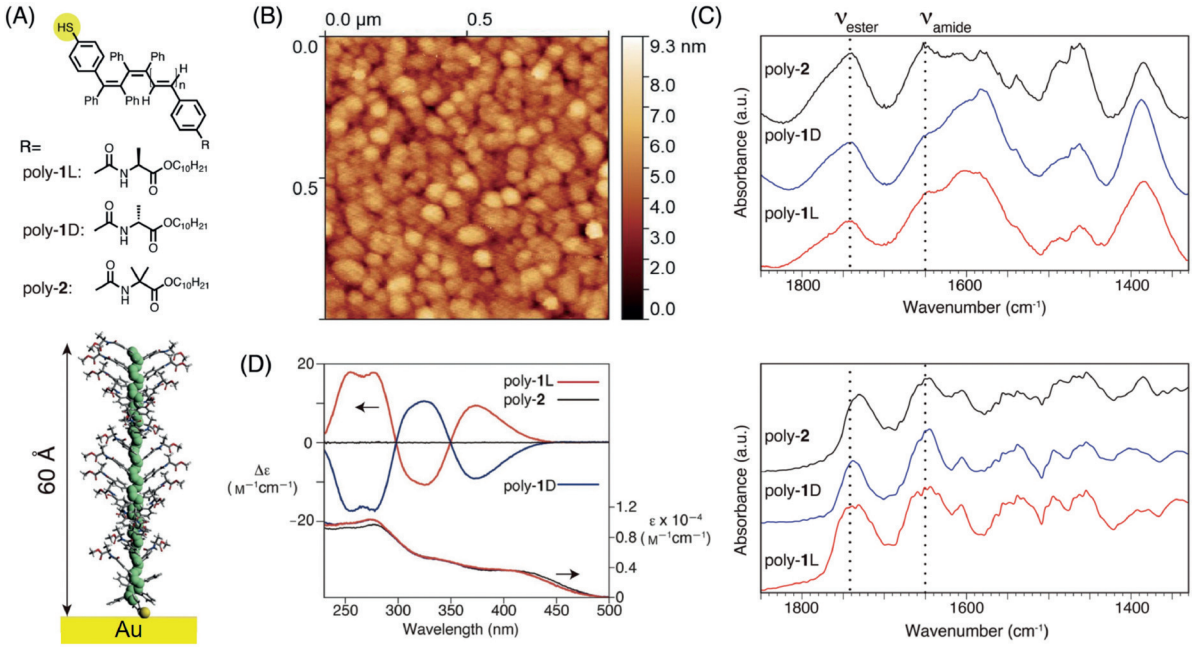

Figure 2. A) The structures of the polymers studied and a scheme showing the binding of the polymers to the gold surface. B) An AFM image of a monolayer of poly-**1**L providing the total thickness (about 6 nm) of the SAM. C) IR spectra recorded for the SAM on gold in reflection mode (top) and drop-cast film in transmittance mode (bottom). D) The CD and absorption spectra of the polymers in THF.

a surface, charge reorganization occurs in the molecule. This spin-dependent charge reorganization (SDCR) affects the reactivity of chiral molecules and contributes to the enantioselectivity in the interaction between chiral molecules.[11] It also affects the interaction of chiral molecules with ferromagnetic surfaces and it can be applied for separating enantiomers.[12]

Here we are presenting the study of the spin filtering properties of a set of helical poly(phenylacetylene)s with a thiol group (-SH) at a terminal end synthesized using a novel living polymerization system.[13] The polymers are poly(4-ethynylbenzoyl-L-alanine decyl ester) (poly-**1**L),[14] poly(4-ethynylbenzoyl-D-alanine decyl ester) (poly-**1**D),[14] and poly(4-ethynylbenzoyl-2-methylalanine decyl ester) (poly-**2**) (Figure 2A; see the Supporting Information for more detail).[15] These polymers are adsorbed as a self-assembled monolayer (SAM), through thiol to gold coated substrates, and the spin filtering properties measured when the electrons are conducted along the backbone of the polymer. Both uniformity of surface and layer thickness are required to achieve stable spin polarization and its measurements. The SAMs of the polymers used here, which have precisely controlled length, are especially suitable for measuring the spin filtering properties.

The poly-**1**L and poly-**1**D have enantiomeric one-handed helical structures that are induced by the enantiomeric chiral side groups, while poly-**2** bearing achiral side groups consists of an equal mixture of right- and left-handed helical structures. The sense of handedness of poly-**1**, right- or left-handed helix, depends on the handedness of the side groups and the solvent used.[16] We investigated how the spin filtering properties depend on the macromolecular helicity and on its inversion when the monolayer is exposed to toluene vapors. The spintronics properties were measured by magnetic conductive probe atomic force microscopy (mcp-AFM), by Hall, and by magnetoresistance devices.

Results and Discussion

The SAMs of the given polymers were characterized by various methods. Figure 2A presents a scheme of the polymer used in this study and Figure 2B shows the atomic force microscope (AFM) image of the SAM of poly-**1**L, which indicates a densely packed monolayer with a thickness of about 6 nm. The monolayer was also characterized by IR spectroscopy in reflection mode (Figure 2C), where one can clearly see the peaks related to the amide and ester at about 1650 and 1736 cm^{-1}, respectively. The spectrum of the monolayer can be compared with transmittance mode spectrum of the drop-cast film (bottom panel). Figure 2D shows the CD and absorption spectra of the polymers in THF at a concentration of about 0.3 mM (0.1 $mg\,mL^{-1}$). As expected, poly-**1**L and poly-**1**D showed characteristic CD peaks in the polymer backbone region (250–450 nm) that are just the mirror image of each other, which can be assigned to the left- and right-handed helical structures, respectively,[16] whereas no CD peak was observed for the optically inactive poly-**2**.

Figure 3 presents the results obtained by magnetic-conductive probe atomic force microscopy (mcp-AFM) where the SAMs of the polymers were absorbed on a ferromagnetic substrate (Ni/Au; see details in the Supporting Information). An electric potential is varied between the substrate and the grounded Pt tip of the AFM and the current through the SAM is measured as a function of the potential

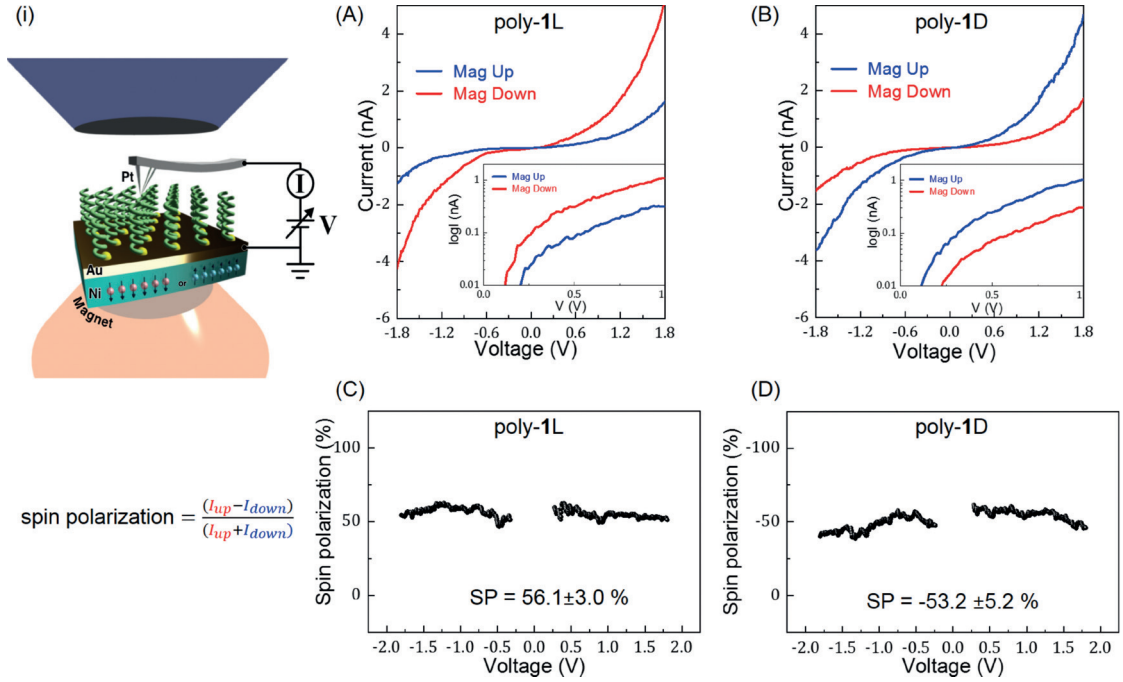

Figure 3. i) Scheme of magnetic conducting probe AFM (mcp-AFM) setup. Panels A and B present the current versus voltage (*I–V*) curves averaged over about 100 scans (see the Supporting Information) and recorded for poly-**1**L and poly-**1**D, respectively, with the magnet north pole pointing up (blue) or down (red). Panels C and D show the calculated spin polarization obtained for poly-**1**L and poly-**1**D, respectively.

for the magnetic substrate magnetized with its north pole up or down. About 100 current–voltage (*I–V*) curves were recorded on each sample and their average is plotted in Figures 3 A and B (see Figure S5 in the Supporting Information). Corresponding semi log plots are presented in the insets, which show the nonlinear dependence of the current on the applied potential and the difference in the threshold for the currents of the electrons with the two-spin polarization. Figures 3 C and D present the spin polarization, SP (%) = $\frac{(I_{up} - I_{down})}{(I_{up} + I_{down})}$ x 100, as a function of the applied voltage, when I_{up} and I_{down} are the currents measured when the magnetic north pole of the substrate is pointing towards or away from the monolayer, respectively. The absolute spin polarization of about 50 % indicates a ratio of about 1:3 in the spin transmission. For the optically inactive poly-**2**, no difference was observed in the averaged *I–V* curves when the magnet north pole points up or down (see Figure S6).

The nonlinear dependence of the current on the applied voltage was observed before in CISS-based mcp-AFM measurements.[1,17,18] It is also clear that a different threshold for charge injection is found for the two spins. The difference is on the order of 100 ± 10 meV, and the spin injected at lower potential depends on the handedness of the polymers. For the poly-**1**L (poly-**1**D), the lower spin corresponds to the magnet pointing up (down), namely the spins injected are polarized antiparallel (parallel) to the electron's velocity. The difference in threshold for injection of the two spins is an indication that during the electron transmission through the polymers, no spin flipping occurs.[19]

There are already indications for the correlation between the optical activity of chiral molecules and the extent of the CISS effect in them.[3,20] This correlation is manifested also in the current study. While the results shown in Figure 3 are obtained when the poly-**1** is initially dissolved in THF, the CD spectrum of poly-**1** changes the sign upon dissolving the polymer in toluene (Figure 4 A). The toluene apparently induces a switch in the handedness of the secondary helical structure of poly-**1** as was verified in the past studies.[16] It is important to appreciate that when a monolayer of the poly-**1**L, made from the THF solution, is exposed to toluene vapors which switch the helicity of the main chain from the left- to right-handed helix, similarly to the process occurring in solution. The spin-dependent current was probed for the poly-**1**L sample before and after toluene treatment. Before the toluene treatment the current is higher when the magnet is down (Figure 3 A), while after being exposed to toluene, the

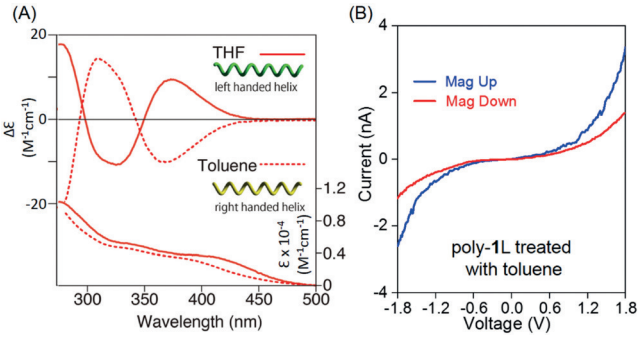

Figure 4. Chemically activated helix switching using toluene vapor. A) CD and absorption spectra of poly-**1**L recorded in THF (solid line) and toluene (dotted line). B) Averaged *I–V* curve of poly-**1**L after toluene treatment when the magnet north pole is pointing up (blue) or down (red).

current is higher for the magnet pointing up (Figure 4B). The results show again the correlation between changes in the CD spectra and the CISS effect. Despite the fact that the monomer has the same chirality, the secondary structure of the polymer depends on the solvent and affects the spin selectivity.

While the mcp-AFM studies described above were performed under ambient conditions, the next set of experiments were done in a solution using the Hall based methods.[6,21,22] These Hall devices are made of a GaN/AlGaN structure with a two-dimensional electron gas (2DEG) interface layer. A common Hall device is applied for monitoring the magnetic field. It is based on a constant current applied between source and drain electrodes. When a magnetic field is acting perpendicular to the surface of the device, as a result of the Lorentz force, electric potential can be measured perpendicular to the source-drain current and to the magnetic field. This potential is the "Hall potential". In the device used here, no external magnetic field is applied, but instead chiral polymers are adsorbed on the surface of the device. Details on the device fabrication and experimental setup are given in the Supporting Information. Two types of measurements were conducted. In the first type, the polymers are adsorbed on the device which is placed within the electrolytic solution using PDMS cell. Externally top gold electrode placed on the top of the solution facing the device and is used to apply the electric field. On the application of the electric field, the polymer is charge polarized and if this charge polarization is accompanied by spin polarization, the spins that are injected from the polymer into the device create a magnetic field which can be monitored by the Hall probes (Figure 5i). The mechanism by which this device is operated is described in detail in Reference [22]. In the second type of experiments, spin-dependent electrochemistry measurements were conducted (Figure 5ii). Here, the Hall device served as the working electrode in a common electrochemical cell which also includes counter and reference electrodes. When the electrochemical cell operates, electrons have to pass through the polymer's SAM on their way from or to the working electrodes. If the current is spin polarized, it will result in Hall potential. Hence, this scheme provides, in addition to the regular C-V plots, the Hall potential dependent on the voltage, that is, an indication for the spin polarization of the current in the electrochemical cell. It is important to appreciate the difference between the two modes of experiments used the Hall device. In the first type of measurement, namely the monitoring of the spin polarization that accompanied the charge polarization, no current is flowing and the spin injected into the Hall device is due to the gate voltage that inject charge, electrons, or holes into the device. In the second type of study, the spin-dependent electrochemistry, a constant current is flowing and the spin associated with this current is monitored.

Figures 5A and B show the Hall signal as a function of time, obtained for poly-**1**L and Poly-**1**D, respectively, when pulses of varying voltage are applied between the gate electrode and the Hall device. Clearly the magnitude of the Hall potential measured correlates with the voltage applied (Figure 5C), and its sign with the handedness of the polymers,

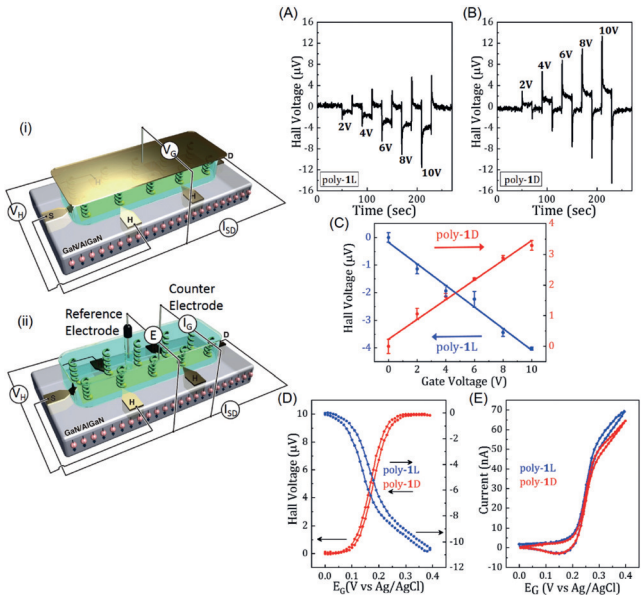

Figure 5. Schematic presentation of the experimental set of Hall measurement in the polarization (i) and electrochemical mode (ii). Hall potential recorded in polarization mode as a function of time for A) poly-**1**L and B) poly-**1**D for various gate pules. C) The Hall voltage as a function of the gate voltage for monolayers of poly-**1**L (blue) or poly-**1**D (red). D) Hall potential recorded in the electrochemical mode as a function of the voltage when the working electrode (the Hall device) is coated with monolayers of poly-**1**L (blue) or poly-**1**D (red). E) The CV curves obtained in the electrochemical process when the working electrode is coated with monolayers of poly-**1**L (blue) or poly-**1**D (red). Note: All the electrochemical measurements were performed using ferrocene as redox probe in water. Pt wire was used as the counter electrode, the drain electrode of the Hall device was used as the working electrode and silver wire used as a reference electrode.

indicating that upon the charge polarization, the polymer is also spin polarized and the spin corresponding to the specific electric pole depends on the handedness of the polymers.

In the electrochemistry related experiments, we measured the spin-selective electron transfer through the polymers. All the electrochemical measurements were performed using ferrocene as a redox probe in PBS buffer. Pt wire was used as the counter electrode, the drain electrode of the Hall device was used as the working electrode, and silver wire used as a reference electrode. Figure 5D shows the Hall potential obtained when the potential in the electrochemical cell was varied between 0 to 0.4 V. The corresponding cyclic voltammetry (CV) plots are shown in Figure 5E. While the CV plots are basically identical for the two enantiomers, the Hall potentials obtained have opposite signs. The small hysteresis observed in the Hall potential plots is an indication for the asymmetry between the spin polarization in the oxidation and reduction currents that may result from differences in the interfaces on the two sides of the polymers, one being the solid substrate and the other the electrolyte.

The ability to apply the polymers for spintronics applications was probed by producing a spin valve which operates because of its magnetoresistance (MR) effect. The device is presented schematically in Figure 6i. A crossbar geometry was employed, with a 2 μm-wide 10/40 nm thick Ti/Au bottom

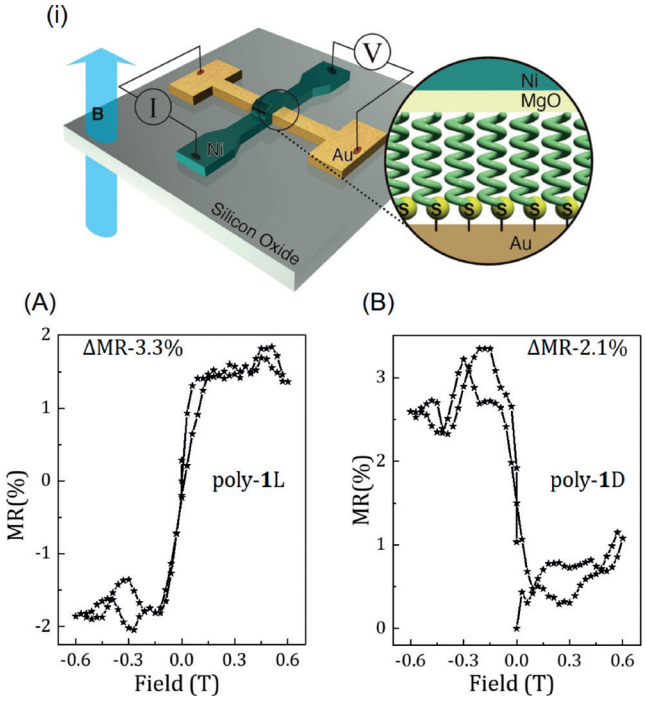

Figure 6. i) Scheme of the four-probe magnetoresistance (MR) measurement setup with bottom gold and top Ni electrode. The inset shows the combination of layers in the MR device. The MR signal of A) poly-**1**L and B) poly-**1**D devices.

electrode was deposited on silicon oxide wafer using optical lithography. On top of this electrode a monolayer of the helical polymer was deposited followed by an insulating buffer layer of 1.5 nm thick magnesium oxide (MgO) and then a ferromagnetic nickel/gold (30/8 nm) 15 μm wide electrode. MR measurements were carried out using a SQUID-MPMS3 (Quantum Design).

The crossbar geometry enables us to measure accurately the resistance of the device by the standard four-probe configuration. The magnetoresistance is defined as $\mathrm{MR}\,(\%) = \frac{(R_H - R_{H=0})}{(R_{H=0})} \times 100$, where R_H is the measured infield resistance and $R_{H=0}$ is the zero-field resistance. Figure 6 presents the MR results measured under ambient conditions with a maximum field of 0.6 T and a constant current of 1 mA, for poly-**1**L and poly-**1**D. The MR plot is asymmetric relative to the field sign, not like in the common MR devices. The reason for the asymmetry is that only one ferromagnetic electrode is used, while the chiral polymers transmit mainly one spin. The MR results are consistent with the other spin-dependent measurements, however the relatively low values probably result from pin holes in the monolayers and from electron scattering. As observed before, there is no simple correlation between the magnitude of the MR signal and the magnitude of the spin polarization as measured by the mcp-AFM. This lack of correlation is because the MR signal depends on the precise geometry, the width of the electrodes used, and the quality of the monolayers, while for the mcp-AFM signal typically only one or very few molecules are measured, and the measurement is much less sensitive to pin-holes in the monolayer. We have observed a clear correlation between the MR studies and the conduction through the polymers measured with the mcp-AFM. For example, in the case poly-**1**L, using the mcp-AFM, the current is lower and the resistance in MR is higher when the magnet is in the up configuration (Figure 6 A).

Conclusion

Past studies on chiral polymers were conducted either on polythiophene[8] or on helical supramolecular π-conjugated nanofibers.[10] In the two cases the polymers were lying on the surface. In the case of polythiophene, the spin polarization was measured to be about 34 % and the magnetoresistance measured was less than 1 %. In the case of the supramolecular nanofibers, very high spin polarization of about 85 % was measured. The difference is attributed to conduction of the current along the polymer backbone, as in the present case, whereas for the supramolecular wires the conduction is across the diameter, and the process involves sequential hopping between the molecules. However, the magnetoresistance in this case was around one order of magnitude lower than in the current study. The low values of the magnetoresistance observed in the past are due to the ill-defined organization of the polymers on the surfaces that allows pin-holes. While in the present study the organization is closely packed and well defined.

The present study confirms that when current is transmitted through the backbone of a chiral polymer the transmission is spin dependent, similar to what is observed when the current is transmitted perpendicular to the backbone. The results observed here are very stable and the variation among various measurements is small. This stability is a result of the uniformity in the length of the polymer and its structure. The correlation between the change in the secondary structure and the spin polarization point to the important role the secondary structure plays in defining the magnitude of the CISS effect. The results also confirm that the spin polarization does not involve spin flipping, and they are consistent with recent findings that the spin polarization is a result of suppression of back scattering for the favored spin, while the other spin is scattered back.[10]

Finally, we see that the common CISS effect is going hand to hand with the spin dependent charge reorganization (SDCR) and with asymmetric MR effects. Hence well controlled chiral polymers are good candidates for organic-spintronic CISS-based applications.

Acknowledgements

E.Z.B.S. and R.N. acknowledge the help of Dr. G. Leitus in conducting the MR measurements. S.M., A.K.M., E.Z.B.S., and R.N. acknowledge the partial support from the Israel Ministry of Science, from Israel Science Foundation, and from the John Templeton Foundation. This work was also supported in part by JSPS KAKENHI (Grant-in-Aid for Specially Promoted Research, no. 18H05209 (K.M. and E.Y.), Grants-in-Aid for Scientific Research (C), no. 18K04723 (T.N.)), and the World Premier International Research Center Initiative

(WPI) of the Ministry of Education, Culture, Sports, Science and Technology (MEXT), Japan.

Conflict of interest

The authors declare no conflict of interest.

Keywords: chirality · electron transport · materials chemistry · polymers · self-assembly

[1] R. Naaman, Y. Paltiel, D. H. Waldeck, *J. Phys. Chem. Lett.* **2020**, *11*, 3660 – 3666.
[2] J. M. Abendroth, N. Nakatsuka, M. Ye, D. Kim, E. E. Fullerton, A. M. Andrews, P. S. Weiss, *ACS Nano* **2017**, *11*, 7516 – 7526.
[3] T. J. Zwang, S. Hürlimann, M. G. Hill, J. K. Barton, *J. Am. Chem. Soc.* **2016**, *138*, 15551 – 15554.
[4] S. Mishra, S. Pirbadian, A. K. Mondal, M. Y. El-Naggar, R. Naaman, *J. Am. Chem. Soc.* **2019**, *141*, 19198 – 19202.
[5] M. Kettner, V. V. Maslyuk, D. Nürenberg, J. Seibel, R. Gutierrez, G. Cuniberti, K.-H. Ernst, H. Zacharias, *J. Phys. Chem. Lett.* **2018**, *9*, 2025 – 2030.
[6] V. Kiran, S. P. Mathew, S. R. Cohen, I. Hernández Delgado, J. Lacour, R. Naaman, *Adv. Mater.* **2016**, *28*, 1957 – 1962.
[7] H. Lu, J. Wang, C. Xiao, X. Pan, X. Chen, R. Brunecky, J. J. Berry, K. Zhu, M. C. Beard, Z. V. Vardeny, *Sci. Adv.* **2019**, *5*, eaay0571.
[8] P. C. Mondal, N. Kantor-Uriel, S. P. Mathew, F. Tassinari, C. Fontanesi, R. Naaman, *Adv. Mater.* **2015**, *27*, 1924 – 1927.
[9] F. Tassinari, K. Banerjee-Ghosh, F. Parenti, V. Kiran, A. Mucci, R. Naaman, *J. Phys. Chem. C* **2017**, *121*, 15777 – 15783.
[10] C. Kulkarni, A. K. Mondal, T. K. Das, G. Grinbom, F. Tassinari, M. F. J. Mabesoone, E. W. Meijer, R. Naaman, *Adv. Mater.* **2020**, *32*, 1904965.
[11] A. Kumar, E. Capua, M. K. Kesharwani, J. M. L. Martin, E. Sitbon, D. H. Waldeck, R. Naaman, *Proc. Natl. Acad. Sci. USA* **2017**, *114*, 2474 – 2478.
[12] R. Naaman, Y. Paltiel, D. H. Waldeck, *Nat. Rev. Chem.* **2019**, *3*, 250 – 260.
[13] T. Taniguchi, T. Yoshida, K. Echizen, K. Takayama, T. Nishimura, K. Maeda, *Angew. Chem. Int. Ed.* **2020**, *59*, 8670 – 8680; *Angew. Chem.* **2020**, *132*, 8748 – 8758.
[14] K. Okoshi, K. Sakajiri, J. Kumaki, E. Yashima, *Macromolecules* **2005**, *38*, 4061 – 4064.
[15] S.-i. Sakurai, S. Ohsawa, K. Nagai, K. Okoshi, J. Kumaki, E. Yashima, *Angew. Chem. Int. Ed.* **2007**, *46*, 7605 – 7608; *Angew. Chem.* **2007**, *119*, 7749 – 7752.
[16] S.-i. Sakurai, K. Okoshi, J. Kumaki, E. Yashima, *J. Am. Chem. Soc.* **2006**, *128*, 5650 – 5651.
[17] R. Naaman, D. H. Waldeck, *Phys. Rev. B* **2020**, *101*, 026403.
[18] S. Mishra, A. K. Mondal, S. Pal, T. K. Das, E. Z. B. Smolinsky, G. Siligardi, R. Naaman, *J. Phys. Chem. C* **2020**, *124*, 10776 – 10782.
[19] D. Nürenberg, H. Zacharias, *Phys. Chem. Chem. Phys.* **2019**, *21*, 3761 – 3770.
[20] B. P. Bloom, B. M. Graff, S. Ghosh, D. N. Beratan, D. H. Waldeck, *J. Am. Chem. Soc.* **2017**, *139*, 9038 – 9043.
[21] A. Kumar, E. Capua, K. Vankayala, C. Fontanesi, R. Naaman, *Angew. Chem. Int. Ed.* **2017**, *56*, 14587 – 14590; *Angew. Chem.* **2017**, *129*, 14779 – 14782.
[22] E. Z. B. Smolinsky, A. Neubauer, A. Kumar, S. Yochelis, E. Capua, R. Carmieli, Y. Paltiel, R. Naaman, K. Michaeli, *J. Phys. Chem. Lett.* **2019**, *10*, 1139 – 1145.

Manuscript received: May 6, 2020
Revised manuscript received: May 28, 2020
Accepted manuscript online: June 13, 2020
Version of record online: July 9, 2020

